A Protein-Based Electrochemical Biosensor Array Platform for Integrated Microsystems

Yue Huang, *Member, IEEE*, Ying Liu, Brian L. Hassler, R. Mark Worden, and Andrew J. Mason, *Senior Member, IEEE*

***Abstract*—This paper elucidates challenges in integrating different classes of proteins into a microsystem and presents an electrochemical array strategy for heterogeneous protein-based biosensors. The overlapping requirements and limitations imposed by biointerface formation, electrochemical characterization, and microsystem fabrication are identified. A planar electrode array is presented that synergistically resolves these requirements using thin film Au and Ag/AgCl electrodes on a dielectric substrate. Using molecular self-assembly, electrodes were modified by nano-structures of two diverse proteins, alkali ion-channel protein and alcohol dehydrogenase enzyme. Electrochemical impedance spectroscopy and cyclic voltammetry measurements were performed to characterize sensor response to alkali ion and alcohol, respectively. This work demonstrates the viability of the electrochemical microsystem platform for heterogeneous protein-based biosensor interfaces.**

***Index Terms*—Biosensors, electrochemistry, enzyme, membrane protein, microelectrode, microsystem.**

I. Introduction

In the post-genomic era, protein arrays have become increasingly attractive for preclinical, toxicological and clinical studies to screen drug candidates, monitor efficacy and toxicity and identify diagnostic markers [1]. Among the dominant drug targets, an estimated 50% are membrane proteins (receptors and ion channels) and 28% are enzymes [2]. Membrane-protein-based biosensors are able to detect drugs, neurotransmitters, hormones, toxins, and inhibitors such as amiloride [3]. Enzyme-based biosensors can monitor the metabolism of a drug or a molecule such as glucose and the corresponding enzyme activity. However, despite the extreme potential of these protein classes, they remain largely undeveloped as sensors agents due to the complexity of their associated interfaces.

Biosensors today predominantly rely on affinity-based interfaces such as nucleic acids, antibodies and antigens, and optical techniques are commonly employed to measure binding of fluorescent tags. Alternatively, sensors utilizing electrochemical techniques have the advantages of direct transduction to electrical signals and reduced interference noise. Furthermore, because electrochemical instrumentation can readily be implemented within CMOS chips, protein-based electrochemical biosensors offer an ideal basis for miniaturization into a microsystem array platform [4]. Electrochemical microsystems have been formed by immobilizing affinity-based bio-recognition interfaces onto CMOS electrodes [5], [6]. However, affinity-based interfaces do not permit continuous operation because the analytes do not disassociate easily from the probe. Alternatively, enzyme and membrane protein interfaces are capable of continuous use and provide label-free monitoring with electrochemical techniques. Enzyme interfaces maintain continuous catalytic activity for amperometric monitoring when immobilized on an electrode by physical trapping or covalent binding [7], [8]. Many membrane proteins can be continuously monitored using a variety of electrochemical techniques and can be immobilized on electrodes using synthetic bilayer lipid membranes (BLM) serving as biomimetic interfaces to circumvent denaturing [9]. The development of a CMOS-based electrochemical microsystem platform that combines membrane-protein and enzyme biointerfaces would enable a new breed of biosensor arrays that are highly valuable for biological research and medical applications. Furthermore, such a platform would open new pathways for biology-to-silicon communication with vast opportunities for future applications. In continuation of previous work [10], [11], this research on microsystem integration fills the gap between heterogeneous protein-based biosensors and CMOS electrochemical instrumentation circuitry by identifying suitable processes for post-CMOS electrode fabrication, bio-interface formation and sensor interrogation. By replacing the protein bio-recognition elements, this model platform can be expanded to tackle a wide range of detection challenges in fundamental biomedical research, medical diagnostics and drug discovery.

II. Microfabricated Electrode Array Design

Combining CMOS electrochemical instrumentation circuitry with IC-compatible electrode arrays introduces the opportunity to realize an electrochemical analysis microsystem with fluid handling structures to facilitate bio-interface formation and test sample delivery, as illustrated in Fig. 1. The electrode array enables a biology-to-silicon interface provided it can simultaneously meet requirements set by 1) IC process compatibility, 2) biointerface self assembly, and 3) electrochemical analysis techniques. This section analyzes the limitations imposed by

Manuscript received November 21, 2011; revised March 21, 2012; accepted April 06, 2012. Date of publication May 24, 2012; date of current version March 07, 2013. This work was supported by the National Science Foundation (DBI-0649847 and IDBR-0756703). This paper was recommended by Associate Editor K. Chakrabarty.

Y. Huang and A. J. Mason are with the Electrical and Computer Engineering Department, Michigan State University, East Lansing, MI 48824 USA (e-mail: abrahuang@gmail.com; mason@msu.edu).

Y. Liu, B. L. Hassler, and R. M. Worden are with the Chemical Engineering and Material Science Department, Michigan State University, East Lansing, MI 48824 USA (e-mail: liuying7@egr.msu.edu; hassler@egr.msu.edu; worden@egr.msu.edu).

Color versions of one or more of the figures in this paper are available online at http://ieeexplore.ieee.org.

Digital Object Identifier 10.1109/TBCAS.2012.2195661

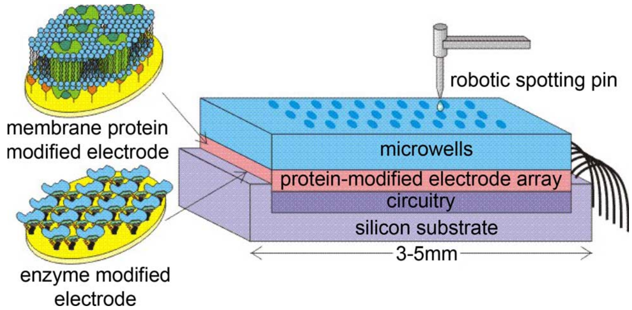

Fig. 1. Protein-based electrochemical biosensor array microsystem concept with fluid delivery to an electrode array on the top of a silicon integrated circuit.

these overlapping requirements and highlights solutions that can be adapted to many electrochemical microsystems.

Instrumentation circuitry supporting many electrochemical methods can be implemented in a low cost integrated circuit (IC) using complementary metal-oxide-semiconductor (CMOS) technology. Many CMOS potentiostats, the core electrochemical biasing circuits, and electrochemical impedance spectroscopy circuits have been reported in the literature, for example [12]–[19]. By integrating electrodes directly on the instrumentation chip, long external connections are eliminated to gain immunity to environmental electromagnetic interference. Through miniaturization, the limits of detection can be extended by improving the signal to noise ratio.

Utilizing photolithography patterning, electrodes suitable for enzyme and membrane protein biosensors can be scaled down to microns, and intricate electrode arrays can be batch fabricated in a planar fashion. CMOS compatible processes such as metal physical vapor deposition, dielectric chemical vapor deposition, wet chemical and plasma dry etching, maintain the reliability of active circuits within the substrate when conducted at temperatures lower than 400°C. These processes have also been used for applications in biology and medicine [20], [21]. However, this microfabrication toolset limits the available electrode materials and structures and, along with biointerface assembly requirements, defines the electrode design space. Based on these requirements, fundamental factors of the electrode array such as electrode configuration, geometry, material, and reliability were studied. Although fully integrated planar 3-electrode electrochemical microsystems have been reported for DNA and bacteria detection [13], [22], no such system has been studied and reported for membrane proteins and enzymes.

A. Electrode Configuration

A typical electrochemical cell consists of three electrodes: working, counter and reference [23]. For sensor applications, only the reactions on the working electrode are of interest. In a two-electrode system, the auxiliary electrode functions as both the reference electrode and the counter electrode, but the potential on the auxiliary electrode tends to be affected by the current passing through it, i.e., the electrode is polarizable. Consequently, the working electrode potential cannot be tightly controlled and could degrade the measurement or even denature the protein interface. Although the polarization effect can be minimized by making the auxiliary electrode significantly larger (e.g., 100x area) than the working electrode, this is counterproductive to realizing a high density working electrode array on the surface of a chip. In contrast, only negligible current passes through the reference electrode in a three-electrode system, providing more reliable potentiostat control with an overall smaller footprint, thus is a more suitable configuration for on-chip bioelectrochemical sensor arrays.

B. Electrode Geometry

The geometrical layout of the working, counter and reference electrodes has a significant effect on sensor performance and microsystem design. Reducing the distance between working and counter electrodes reduces solution resistance and thus speeds up charging of the double layer capacitance, providing faster steady-state sensor response. Reducing the distance between the reference electrode and the working electrode minimizes the uncompensated portion of IR (current-resistance product) loss to provide tighter control of the working electrode potential.

As the size of working electrodes scale down, the miniaturization of reference electrodes is also desired. In practice, it is difficult to fabricate a reliable yet small reference electrode, and it is difficult to place the reference electrode close to the working electrode due to material and fabrication complexity. A solution is placing the reference electrode where the counter-to-working electrode current is low to help minimize the current contribution of IR loss. Alternatively, the IR loss constant can be determined prior to a live measurement and then compensated through the potentiostat, allowing the reference electrode to be placed away from the working electrode.

For this work, the electrode size was designed to match the current readout capability of a bench top instrument, but it can be scaled down to generate current in a range suitable for a CMOS current readout circuit. From an electrochemistry point of view, as the electrode size scales down to a dimension smaller than the diffusion layer (i.e., microelectrode) the faradic current (response) portion of the total current is greater, resulting in larger signal-to-noise ratio and improving the limits of detection, along with other advantages [23], [24]. On the other hand, smaller electrodes exhibit more variability between electrodes and more error due to interference. This tradeoff must be addressed to meet application-specific goals.

C. Electrode Materials

The electrode material for working and counter electrodes must be chosen for compatibility with microfabrication, protein interface formation and the chemistry of testing environment. Gold is an ideal candidate: it is chemically inert; it can be readily deposited in thin films and patterned using photolithography; it forms a strong covalent bond to thiols commonly used in biointerfaces; and it is suitable for both working and counter electrodes to simplify the fabrication process.

For the reference electrode, Ag/AgCl is preferable over other candidates due to its biocompatibility and ease of microfabrication. A thin silver film can be achieved by physical vapor deposition and then chlorinated to form Ag/AgCl using wet chemistry, electrochemistry or Cl plasma. AgCl formed in Cl plasma was reported to be uniform and densely packed [25]. Membrane coatings over Ag/AgCl electrodes have been utilized

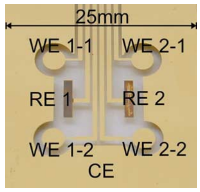

Fig. 2. Microfabricated electrodes with 2×2 working electrode array and Ag/AgCl reference electrodes.

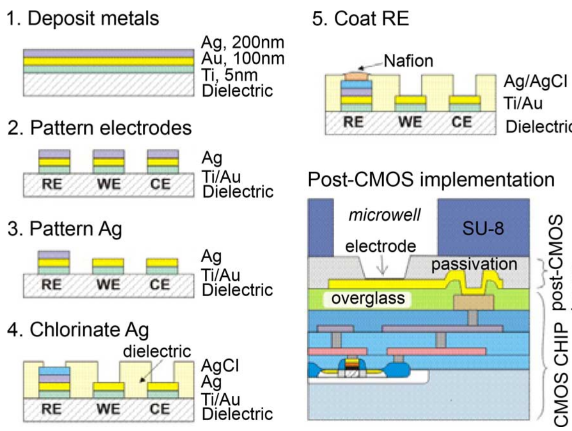

Fig. 3. Fabrication sequence for integrated electrochemical electrode arrays with embedded Ag/AgCl reference electrodes and an illustration of a post-CMOS implementation.

to mimic the glass frit of a conventional reference electrode, providing a diffusion barrier, electron/proton pathway and hydrolyzation-protection [26]–[28]. For example, a Nafion membrane allows only protons (H^+) to pass through, maintaining a conductive electrode-solution interface while detaining Cl^- and Ag^+ ions. Nafion was found to stabilize the reference electrode potential by blocking interfering Cl^-, Br^- and S^{2-} ions. Strictly speaking, such electrodes are quasi-reference electrodes (QRE), because their potential could be affected by pH or other interferences.

D. Planar Electrode Array Fabrication

As an intermediate step toward full system integration, planar electrode arrays were microfabricated through an IC compatible process on SiO_2 passivated silicon substrates that represent the surface dielectric material of a typical CMOS chip. Fig. 2 shows the microfabricated 3-electrode system with gold working electrodes, Nafion-coated Ag/AgCl QREs, and a surrounding shared gold counter electrode. The 2×2 working electrode array, consisting of 1 mm radius disk electrodes, was grouped in pairs that share a Ag/AgCl reference electrode. The traces leading to the working electrodes were passivated, leaving a well confined surface area of $3.14\ \mathrm{mm}^2$.

The post-CMOS compatible electrode array fabrication process consists of five steps shown in Fig. 3. In the first step, thin films of 30 nm Ti, 100 nm Au and 200 nm Ag were deposited onto the SiO_2 substrate using an Edward Auto306 thermal evaporator. In the second step, the electrode areas were patterned by spin coating, exposing, developing and post-development baking of photoresist. The positive film masks used for photolithography were generated through a 3556 dpi Scitex Dolev 450 Immagesetter (Infinity Graphics, Okemos, MI). The array was then dipped into silver etchant $(NH_4OH : H_2O_2\ 1:1)$, gold etchant $(I_2 : KI : H_2O\ 4:1:4)$, and titanium etchant $(HF : H_2O\ 1:9)$ sequentially, leaving all metals on all electrode sites. In step 3, unwanted Ag on the working and counter electrodes was removed by masking the reference electrode sites with photoresist before dipping into silver etchant. In step 4, after a passivation layer was patterned to expose the electrode areas, a AgCl layer was formed over the reference electrodes by oxidizing Ag in 10 mM $FeCl_3$ solution to chlorinate the surface while preserving a thin Ag layer underneath and creating the Ag/AgCl interface. The underlying Au layer provides electrical conduction. After chlorinization, the AgCl surface was rinsed with saturated KCl and DI water to remove absorbed Fe^{3+} and Fe^{2+} and then dried with nitrogen. In step 5, AgCl was coated with a Nafion polymer layer (Nafion 117 5% solution, DuPont) that was cured at 120°C for 1 hr [29]. Following electrode array fabrication, a polydimethylsiloxan (PDMS) mold was attached to protect reference and counter electrodes during self-assembly of biointerfaces on individual working electrodes, and the PDMS mold was removed afterward. Fig. 3 also illustrates the implementation of an electrode array on a CMOS chip, details of which can be found in [30]. Briefly, a post-CMOS metal electrode is formed on CMOS overglass with a metal trace connecting to CMOS circuitry via an overglass opening. A passivation layer is then applied on top of post-CMOS electrodes and defines the electrode area.

III. Molecular Self-Assembled Membrane Protein Sensor Platform

A model electrochemical sensor array platform was implemented by incorporating an enzyme-based alcohol sensor and an ion channel-based alkali sensor. Because alcohol and alkali ions, including sodium and potassium, are reported to have an effect on blood pressure [31], [32], this model sensor array could aid in the study and treatment of cardiovascular disorders, diabetes and related complications. The theory, methods and materials for membrane sensors and enzyme sensor are presented in this section and Section IV, respectively.

A. BLM Formation

Cell membranes are one of the major structural components of biological cells, and they are composed of lipids with membrane proteins and other biomacromolecules interposed between them. Systems that can mimic biological cell membranes and their functionality have great potential for biosensor applications and investigations of fundamental biomolecular behavior [33], [34]. To mimic cell membranes, supported bilayer lipid membranes (sBLMs) have been formed on glass, silica and metal surfaces [35], [36]. Such sBLMs enabled researchers to probe lipid properties including phase transition, lateral diffusion, permeation and lipid protein interactions. However, a major drawback of sBLMs is that they lack a well defined space between the electrode and the membrane, limiting their utility, especially for the study important membrane transport functions. To overcome this drawback, new approaches involving the use of tethering molecules that act as cushions the BLM and the electrode are becoming popular [37]–[42]. A

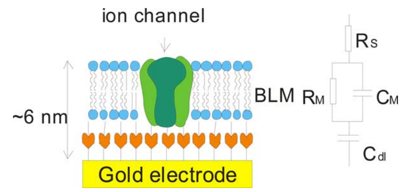

Fig. 4. Ion channel protein embedded in tBLM on a gold electrode and the equivalent circuit model.

tethered bilayer lipid membrane (tBLM) architecture separates the BLM from the electrode surface using a hydrophilic spacer molecule that provides an ion reservoir needed to measure ion channel activity. For studying transmembrane proteins properties, tBLMs should ideally possess the following characteristics: (1) a fluid yet highly insulating lipid core, (2) a well-defined functional space on each side of the membrane, (3) a high degree of mechanical, chemical and biochemical stability, (4) accessibility to electrical measurements, and (5) ease and reliability of production.

B. Membrane Protein Embeded TBLM Sensor Platform

The tBLM-based biomimetic sensor platform is able to incorporate a wide variety of natural and synthetic transmembrane/membrane proteins. Among these, ion channels are transmembrane proteins that facilitate the diffusion of ions across biological membranes by providing a highly conducting and hydrophilic pathway across the hydrophobic membrane interior. Recently, numerous tBLM systems with good characteristics for studying ion channel proteins have been reported [38], [42]–[46]. The Randle's equivalent electrical model shown in Fig. 4 is typically used to describe a tBLM sensor structure, where $\mathrm{C_M}$ represents the degree of surface coverage of the tBLM and $\mathrm{R_M}$ represents the ability of the tBLM to impede ion transport. Ion channel proteins selectively allow the transport of ions across the BLM, thereby altering $\mathrm{R_M}$. The model also includes a double layer capacitance $\mathrm{C_{dl}}$ and solution resistance $\mathrm{R_s}$. Electrochemical impedance spectroscopy (EIS) is often used to characterize tBLM interfaces and obtain values for $\mathrm{R_M}$ and $\mathrm{C_M}$ that indicate the insulating nature of the tBLM. In this technique, a tBLM is assembled on the surface of a metal electrode and the impedance is then measured as a function of frequency. Ion channel protein incorporated in the tBLM will alter the impedance spectrum through changes in $\mathrm{R_M}$, and activity of ion channels can be monitored by observing $\mathrm{R_M}$ over time.

C. Ion-Channel Protein TBLM Alkali Sensor

An alkali sensor can be formed by embedding gramicidin, a dimeric membrane protein that selectively transports alkali metal ions, into the tBLM. The resulting interface will ensure that only alkali ions such as sodium and potassium pass through the BLM. The concentration of alkali analyte in the test solution will reflect proportionally in the membrane parameter $\mathrm{R_M}$.

Following published procedures [42], [44], an insulating tethered lipid bilayer incorporating an ion channel protein was assembled on the gold electrode. Briefly, a self-assembled monolayer (SAM) of DPPTE (1 mM) was deposited on an ultra flat gold substrate by placing the gold substrates in an ethanolic solution of tethering lipids for 1 h. The SAM modified gold electrode was then washed with ethanol to remove unadsorbed lipids and dried under nitrogen. A lipisome solution of DOPC (1 mM) in HEPES buffer (pH7.4) was then put on top of this gold electrode for 24 hrs, resulting in the formation of tethered lipid bilayer membrane. Gramicidin insertion into the tBLM was accomplished by adding its ethanolic stock solution to give the desired gramicidin concentration in the electrolyte solution.

D. Experimental Setup

Ellipsometric measurements were carried out using rotating analyzer ellipsometer (Model M-44; J.A. Woollan Co. Inc., Lincoln, NE) running WVASE32 software. The SAM thickness values were determined using 44 wavelengths between 414.0 and 736.1 nm. The angle of incidence was 75°, and the refractive index of the SAM was assumed to be described by $\mathrm{n} = 1.5$ and $\mathrm{k} = 0$. The advancing contact angle for the tethering lipid SAM was measured by pendant drop shape analysis using a software-controlled SEO Contact Angle Analyzer (Phoenix 450, Surface Electro Optics Corporation Ltd., Korea). Electrochemical measurements were performed using a CHI660B electrochemical workstation. EIS was carried out in 100 mM KCl solution at 0 V DC potential and a 5 mV sinusoidal signal over a frequency range of 0.01 to 10,000 Hz. Electrochemical parameters were calculated by fitting a Randle's equivalent circuit, $\mathrm{R_s}$, $\mathrm{R_M}$, $\mathrm{C_M}$ and $\mathrm{C_{dl}}$ to the impedance data, using Z-view software (Scribner Associates, Southern Pines, NC). CV was performed using 1 mM $\mathrm{K_3Fe(CN)_6}$ as a redox species, with 100 mM KCl as supporting electrolyte. The potential was cycled in a range of 500 mV to -200 mV relative to a Ag/AgCl reference electrode at a scan rate of 50 mV/s. A commercial reference electrode was used to maintain consistency across experiments.

IV. Enzyme-Based Bioelectronic Interface Platform

A. Enzyme Immobilization and Sensor Platform

Enzyme interfaces have been widely used to construct biosensors [8], [47], [48]. This type of bioelectronic interface allows electron exchange between an enzyme and an underlying electrode. *Oxidoreductases*, including dehydrogenase, enzymes are of particular interest for bioelectronic applications because they catalyze reactions that involve direct electron transfer. Enzymes can be immobilized by polymer matrices or by molecular self-assembly using enzyme cofactors and electron mediators. The enzyme cofactor is a specific dinucleotide that can diffuse and embed into the enzyme to enable charge turnover. The cofactor disassociates with the enzyme after acquiring charge. Electron mediators are smaller redox reversible molecules that facilitate electron transfer from the reactive sites of the enzyme to the electrode and reduce the overpotential.

Rather than requiring the enzyme cofactor or electron mediator to be prepared within the test solution, a self-contained structure can co-immobilize the cofactor and mediator with the enzyme on the electrode, providing continuous measurement by

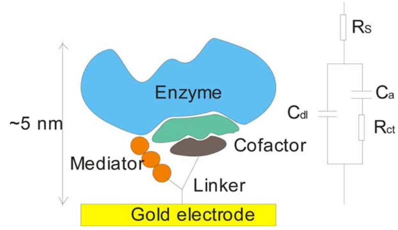

Fig. 5. Enzyme immobilized on a gold electrode with heterotrifunctional linker, electron mediator and cofactor, and the equivalent circuit model.

recycling the mediator and cofactor *in situ*. Zayats *et al.* developed a linear molecular chain consisting of an electrode, a mediator, a cofactor, and an enzyme [8]. We introduced an electron transfer scaffold using a heterotrifunctional linking molecule (i.e., cysteine, Cys) [48]. As shown in Fig. 5, the electron mediator and cofactor were bound to opposite branches of the linking molecule, allowing greater flexibility in scaffold formation and permitting the use of electron mediators having a single reactive group. In the equivalent circuit model shown in Fig. 5, R_{ct} and C_a are the charge-transfer resistance and the adsorption pseudocapacitance, respectively.

B. Secondary Alcohol Dehydrogenase Alcohol Sensor

Secondary alcohol dehydrogenase (2° ADH) from *Thermoanaerobacter ethanolicus (T. ethanolicus)* was produced using Escherichia coli (DH 5α pADH B1 M1-kan) and then purified as previously described [48]. The gold electrodes were soaked in a 0.1 M aqueous solution of cysteine (Cys) for 1 h at room temperature ($25 \pm 2^\circ C$) and then thoroughly rinsed with water to remove weakly adsorbed Cys. The Cys-modified gold electrodes were incubated for 2 h in a 0.1 M phosphate buffer solution (PBS), pH 7.4, containing 100 μM toluidine blue O (TBO) in the presence of 2 mM n-hydroxysuccinimide (NHS) and 2 mM 1-ethyl-3-(3-dimethylaminopropyl) carbodiimide (EDC) to covalently link TBO to the Cys monolayer (Cys-TBO). The Cys-TBO-modified electrodes were soaked in a 10 mM aqueous solution of .polycation poly(ethylenimine) (PEI) solution containing 0.1 M NaCl, pH 7.0, forming an Cys-TBO-PEI-modified interface. A 5 mM aqueous solution of 3-carboxyphenyl boronic acid (CBA) solution was activated at room temperature in the presence of 2 mM NHS and 2 mM EDC in PBS for 2 h. The activated CBA was then reacted with the Cys-TBO-functionalized electrodes for 1 h at room temperature, resulting in an amide linkage between the CBA and the amine group of the Cys. The resulting Cys-TBO-PEI-CBA-modified electrodes were reacted with a 1 mM solution of $NADP^+$ in PBS, pH 7.4, for 1 h. To bind 2° ADH, the MPA-TBO-PEI-$NADP^+$ functionalized electrodes were incubated with $4.4\ mg\ mL^{-1}$ 2° ADH in 0.1 M PBS, pH 7.4, for 1 h at room temperature and cross-linked with 25% (v/v) glutaric acid in water for 20 min. The resulting 2° ADH-modified interfaces were used for the biocatalytic oxidation of 2-propanol.

C. Experimental Setup

Cyclic voltammetry (CV), chronoamperometry, and constant potential amperometry were performed in a grounded Faraday cage using a CHI660B electrochemical workstation connected to a personal computer. Chronoamperometric experiments were conducted by stepping the potential of the working electrode from $-200\ mV$ to 400 mV, triggering oxidation of 2-propanol near the electrode. Origin (Version 7.6, OriginLab, Northampton, MA) was used to fit kinetic models to the resulting current versus time data. Constant potential amperometry experiments were conducted by holding the potential constant at 400 mV, which caused oxidation at the interface. CV experiments were conducted by sweeping the potential of the working electrode between $-200\ mV$ and 400 mV at a scan rate of $100\ mV \cdot s^{-1}$, causing analyte near the electrode to be oxidized in the positive direction and reduced in the reverse direction. Electrochemical measurements were recorded in 0.1 M PBS, pH 7.4, at room temperature for 2° ADH. A commercial reference electrode was used along with the on-chip QRE to monitor QRE potential throughout the experiments.

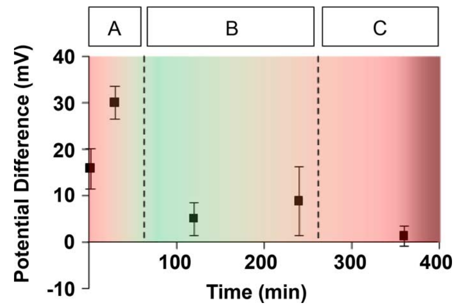

Fig. 6. Potential difference between microfabricated planar on-chip Ag/AgCl reference electrode and commercial Ag/AgCl electrode ($N = 8$).

V. Results and Discussion

A. Microfabricated Electrode Array Characterization

After fabrication, the electrode array was characterized before it was modified by biointerfaces. First, the Ag/AgCl QREs were examined by measuring the potential difference to a commercial Ag/AgCl reference electrode in a 3M KCl solution over time. As shown in Fig. 6, the potential difference rose quickly from zero to a maximum 30 mV and then decayed slowly until it diminished after 6 hrs. The potential difference fluctuation is largely due to the Nafion layer and is associated with the membrane potential. By visual inspection, cracks were observed to develop as the experiment progressed. The process can be roughly partitioned into three regions. Initially, the Nafion membrane was a non-conducting dry film, acting as an open circuit with no potential difference. In region A, sulfonic acid sites of Nafion were gradually hydrated, allowing protons to tunnel through [49] and the Nafion to become conductive. In region B, the membrane experienced a relatively slow stabilization process where the hydration progress was presumably being completed. In region C, hydrolysis became detrimental and resulted in gradually developing cracks. The corrupted membrane exposed AgCl directly to the outer solution, turning the RE into a bare Ag/AgCl QRE, with potential equal to a commercial RE (with the difference of glass frit membrane potential). This experiment indicated that the planar RE was useful for a limited lifetime. However, forming reliable miniaturized reference electrodes remains a challenge, and more sophisticated coatings, diffusion barriers or fortified membranes, as well as new materials are currently being investigated. Shinwari *et al.*. reviews recent advances in REs and compares their performance [50]. $\mathrm{IrO_x}$ is an alternative to Ag/AgCl that is insoluble in aqueous solutions, easy to fabricate and has a long lifetime, making it a promising candidate for microsystems [51], [52].

Each working electrode from a set of arrays was also characterized before modification. The experiments were conducted in potassium ferricynide $(\mathrm{K_3Fe(CN)_6})$ solution by using a CHI 660B electrochemical workstation (CH Instrument, Austin, Texas). The obtained voltammogram showed only small variances between working electrodes. The after-cathodic-peak variance in the diffusion-limited regime was due to convection and is therefore negligible. Thus, the working electrodes of the array were regarded as well matched and suitable for modification with bio-interfaces.

B. Ion-Channel Alkali Ion Biosensor Characterization

The tethering lipid SAM was characterized using contact angle measurement, ellipsometry, EIS and CV. Ellipsometry indicated that the tethering lipid SAM had a thickness of 2.7 ± 0.1 nm, which is comparable to the length of tethering lipid molecule. The SAM exhibited advancing and receding contact angles of $109 \pm 3°$; and $105 \pm 3°$ respectively, consistent with formation of a uniform, ordered, hydrophobic SAM film on the gold substrate. From EIS studies, the capacitance of a bare gold surface and the capacitance of tBLM were found to be $100\ \mu\mathrm{F} \cdot \mathrm{cm}^{-2}$ and $0.89\ \mu\mathrm{F} \cdot \mathrm{cm}^{-2}$, respectively. The drop in capacitance values by two orders of magnitude demonstrated that the electrode surface was covered by tBLM. The resistance of the tethering lipid SAM was found to be $7\ \mathrm{K\Omega} \cdot \mathrm{cm}^2$, which increased to $199\ \mathrm{K\Omega} \cdot \mathrm{cm}^2$ after deposition of the upper leaflet of the tBLM. After tBLM formation, gramicidin ion channels were incorporated in BLM by maintaining $1\ \mu\mathrm{M}$ protein in the electrolyte solution. The incorporation continued for one hour before testing. Since gramicidin can transport both potassium and sodium ions almost equally, potassium was elaborated to characterize this alkali sensor.

The impedance spectrum shown in Fig. 7 was measured in the presence of KCl up to 150 mM, which covers the typical potassium concentration in blood (3.5 mM to 5.2 mM) and urine (25 mM to 125 mM) and the typical blood sodium concentration (136 mM to 145 mM).. In the $\mathrm{R_M}$ dominated frequency range shown in the Fig. 7 inset, the magnitude of impedance decreases as KCl concentration increases. One step further, the membrane resistance $\mathrm{R_M}$ was extracted from Fig. 7 impedance data using Z-View and plotted versus KCl concentration, shown in Fig. 8. The inset plot of Fig. 8 indicates the high linearity of $\mathrm{R_M}$ in the blood potassium concentration range, where a $\mathrm{K^+}$ sensitivity of $-69.36\ \mathrm{k\Omega} \cdot \mathrm{mM}^{-1}$ was obtained.

To determine the limit of detection (LOD), multiple measurements were performed in a buffer solution without any ions. The standard deviation of $\mathrm{R_M}$ was calculated to be $48.41\ \mathrm{k\Omega}\ (\mathrm{n} = 3)$, and the LOD was calculated as three times the standard deviation, $145.23\ \mathrm{k\Omega}$ Using the absolute value of sensitivity,

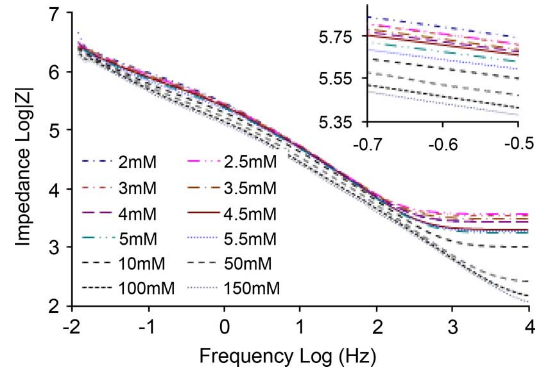

Fig. 7. Impedance spectrum of gramicidin embedded tBLM in presence of KCl. Inset is a magnified plot of the $\mathrm{R_M}$-dominate frequency range.

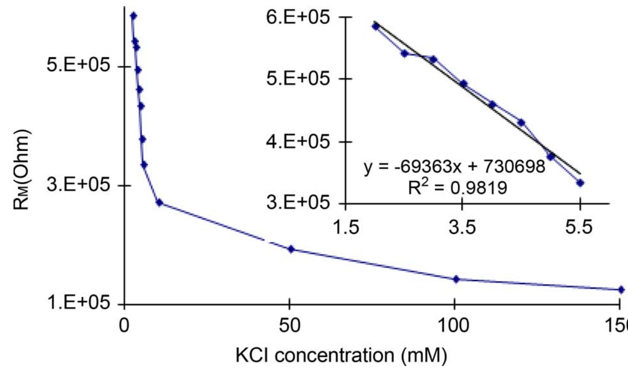

Fig. 8. Membrane resistance RM versus KCl concentration. Inset is magnified plot in concentration range of blood potassium.

TABLE I
COMPARISON OF BLM POTASSIUM SENSORS

	BLM-ion channel	*K^+ Range (mM)*	*Sensitivity*	*LOD (mM)*
This work	tBLM-Gramicidin	2 to 150	-69.36 $\mathrm{k\Omega \cdot mM^{-1}}$	2.12
[43]	sBLM-Valinomycin	2.5 to 130	N/A	N/A

$69.36\ \mathrm{k\Omega} \cdot \mathrm{mM}^{-1}$, the LOD in the range of 2 mM to 5.5 mM is 2.12 mM.

Selectivity was studied by performing CV experiments on tBLMs embedded with gramicidin in different ion solutions. Membrane resistance found to remain constant in barium chloride, calcium chloride and ammonium chloride solutions, which indicates that the interface is selective in the ions it will transport. Furthermore, the gramicidin tBLM interface was observed to exhibit negligible response to alcohol (the target analyte for the enzyme interface). This was studied by increasing ethanol concentration from 0.1% to 0.2% (v/v) in 150 mM KCl solution; the resulting $\mathrm{R_M}$ change of only $5.6\ \mathrm{k\Omega}$ is significantly less than the measured LOD and is therefore negligible.

The performance of the tBLM alkali sensor in measuring potassium ion concentration is summarized in Table I and compared with a reported potassium sensor [53]. This model membrane protein interface demonstrates the potential of the protein-based electrochemical biosensor array platform introduced in this paper. The tBLM sensor can be easily adapted to measure the activity of several other membrane transport proteins or ions by embedding different ion channel and pore-forming proteins into the tBLM interface using similar protocols.

C. Secondary Alcohol Dehydrogenase Alcohol Sensor Characterization

A chronoamperometry experiment was carried out to determine the enzyme surface coverage of the Cys-TBO-NADP$^+$-2° ADH-modified electrode in the presence of 2-propanol following a step change in potential from -200 to 400 mV. The resulting Γ value of $2.1 \pm 0.1 \times 10^{-11}$ mol $\cdot$ cm^{-2} represents the surface density of functional bioelectronic complexes able to achieve multistep electron transfer between the enzyme and electrode. This Γ value is comparable to that measured for a Cys-TBO-NADP$^+$-2° ADH-modified gold coated silicon wafer (2.1×10^{-11} mol cm^{-2}) [48].

Fig. 9 shows cyclic voltammograms of the Cys-TBO-NADP + -2° ADH-modified electrode at varying 2-propanol concentrations. The peak anodic current varies linearly with 2-propanol concentration, shown in the inset of Fig. 9, indicating the interface can function well as a 2-propanol biosensor. The slope of the response curve, 3.9 ± 0.1 μA $\cdot$ mM^{-1} $\cdot$ cm^{-2}, represents the biosensor's sensitivity. At higher concentrations, the anodic current reaches a saturation value ($I_{cat}^{sat} = 207.2 \pm 5.0\ \mu\mathrm{A} \cdot \mathrm{cm}^{-2}$). Using this value, the maximum turnover rate ($TR_{\max}$) can be determined from [54]

$$TR_{\max} = \frac{I_{cat}^{sat} - I_0}{nFA\Gamma} \tag{1}$$

where I_0, the background current, is the y-intercept of the response curve. The $TR_{\max}$ value represents the number of molecules of 2-propanol oxidized per 2° ADH molecule per second. Using (1), the $TR_{\max}$ was calculated to be $26.3 \pm 1.4\ \mathrm{s}^{-1}$. To evaluate the reproducibility of the method, three bioelectronic interfaces were fabricated, and the current was measured for each at multiple 2-propanol concentrations. For 5, 15 and 25 mM, the results showed standard deviations of 0.3% ($n = 3$), 1.3% ($n = 3$), and 1.3% ($n = 3$), respectively, demonstrating good reproducibility.

Fig. 10 shows responses of the Cys-TBO-NADP$^+$-2° ADH-modified electrode to 500 μM steps of increasing 2-propanol concentration in PBS, pH 7.4, under constant stirring at a constant potential of 400 mV. The resulting calibration curve (not shown) indicates a linear response to alcohol concentrations between 0.5 mM and 2 mM and a sensitivity of 3.5 ± 0.4 μA $\cdot$ mM^{-1} $\cdot$ cm^{-2}. The limit of detection was determined to be 100 μM, which is sufficient for blood alcohol content determination. This model enzyme bioelectronic interface demonstrates the potential of the protein-based electrochemical biosensor array platform introduced in this paper.

Sensor lifetime is an important property for continuous use applications. The reported lifetime of redox enzyme sensors include a shelf life of up to 520 days [55] and a usage time of up to 25 days [56]. Sensors using tBLM and membrane proteins are being actively researched today, but the shelf life and functional lifetime of tBLM before or after protein insertion have not been reported in literature. The relationship between electrode size and lifetime with respect to operating conditions and storage environment are subjects of ongoing research.

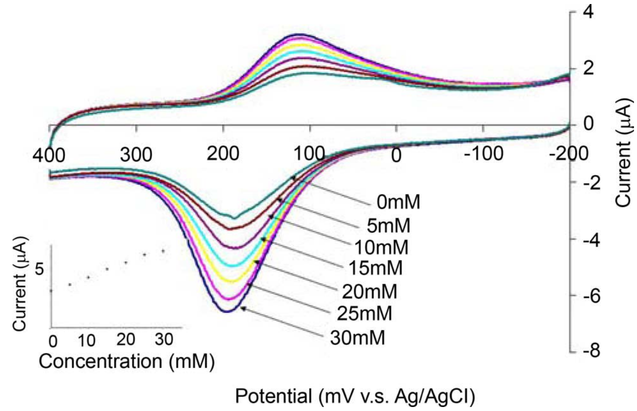

Fig. 9. Cyclic voltammograms of the Cys-TBO-NADP$^+$-2° ADH-functionalized electrode in the presence of different concentrations of 2-propanol from 0 to 30 mM. The data were recorded in room-temperature PBS at a potential scan rate of 100 mV s^{-1}.

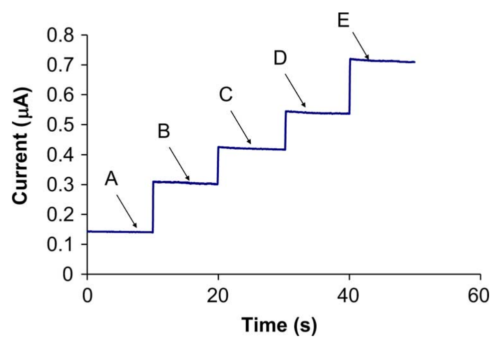

Fig. 10. Constant potential amperometric measurements for the Cys-TBO-NADP$^+$-2° ADH-functionalized electrode in the presence of different concentrations of 2-proponol at a potential of 400 mV (A) 0, (B) 0.5, (C) 1.0, (D) 1.5, and (E) 2.0 mM.

VI. Conclusions

This paper introduced a set of technologies for assembly of heterogeneous protein biosensors within a microsystem platform. A scalable, CMOS chip compatible electrode array was microfabricated to demonstrate its capability to accommodate membrane protein and enzyme biosensor interfaces. A self-assembled biomimetic membrane was formed on the electrode array, followed by insertion of gramicidin, an ion channel protein, and impedance spectroscopy verified the selective detection of potassium ions. In parallel, a secondary alcohol dehydrogenase enzyme was immobilized and probed by amperometry to exhibit an alcohol sensor response. These two model interface verify the viability of the reported fabrication technologies and represent only the beginning of the platform's full potential. By exchanging the proteins and by increasing the array density, this electrochemical sensor platform is capable of incorporating multiple heterogeneous proteins for parallel measurement in applications such as high throughput drug screening and clinical diagnostics. Moreover, this platform is a milestone toward integrating protein-based electrochemical biosensor arrays and microelectronic instrumentation into highly functional monolithic microsystems.

References

[1] A. Lueking, D. J. Cahill, and S. Mullner, "Protein biochips: A new and versatile platform technology for molecular medicine," *Drug Disc. Today*, vol. 10, pp. 789–794, Jun. 2005.

[2] J. Drews, "Drug discovery: A historical perspective," *Science*, vol. 287, pp. 1960–1964, Mar. 2000.

[3] P. Yin, C. J. Burns, P. D. J. Osman, and B. A. Cornell, "A tethered bilayer sensor containing alamethicin channels and its detection of amiloride based inhibitors," *Biosens. Bioelectron.*, vol. 18, pp. 389–397, Apr. 2003.

[4] M. Trojanowicz, "Miniaturized biochemical sensing devices based on planar bilayer lipid membranes," *Fresenius' J. Anal. Chem.*, vol. 371, pp. 246–260, Sep. 2001.

[5] C. Stagni, C. Guiducci, L. Benini, B. Ricco, S. Carrara, B. Samori, C. Paulus, M. Schienle, M. Augustyniak, and R. Thewes, "CMOS DNA sensor array with integrated A/D conversion based on label-free capacitance measurement," *IEEE J. Solid-State Circuits*, vol. 41, pp. 2956–2964, 2006.

[6] A. Hassibi and T. H. Lee, "A programmable $0.18\ \mu\mathrm{m}$ CMOS electrochemical sensor microarray for biomolecular detection," *IEEE Sensors J.*, vol. 6, pp. 1380–1388, 2006.

[7] S. Cosnier, "Biomolecule immobilization on electrode surfaces by entrapment or attachment to electrochemically polymerized films. A review," *Biosens. Bioelectron.*, vol. 14, pp. 443–456, May 1999.

[8] M. Zayats, E. Katz, and I. Willner, "Electrical contacting of flavoenzymes and $\mathrm{NAD(P)(+)}$-dependent enzymes by reconstitution and affinity interactions on phenylboronic acid monolayers associated with Au-electrodes," *J. Amer. Chem. Soc.*, vol. 124, pp. 14724–14735, Dec. 2002.

[9] F. Henn and T. Thompson, "Synthetic lipid bilayer membranes," *Annu. Rev. Biochem.*, vol. 38, pp. 241–262, Jun. 1969.

[10] P. Kim, N. Kohl, B. Hassler, N. Dotson, A. Mason, R. M. Worden, and R. Ofoli, "An electrochemical interface for integrated biosensors," in *Proc. IEEE Int. Conf. Sensors*, Toronto, ON, Canada, 2003, pp. 1036–1040.

[11] C. Yang, Y. Huang, B. L. Hassler, R. M. Worden, and A. J. Mason, "Amperometric electrochemical microsystem for a miniaturized protein biosensor array," *IEEE Trans. Biomed. Circuits Syst.*, vol. 3, pp. 160–168, Jun. 2009.

[12] R. J. Reay, A. F. Flannery, C. W. Storment, S. P. Kounaves, and G. T. A. Kovacs, "Microfabricated electrochemical analysis system for heavy metal detection," *Sens. Actuators B, Chem.*, vol. 34, pp. 450–455, Aug. 1996.

[13] A. Frey, M. Schienle, C. Paulus, Z. Jun, F. Hofmann, P. Schindler-Bauer, B. Holzapfl, M. Atzesberger, G. Beer, M. Fritz, T. Haneder, H. C. Hanke, and R. Thewes, "A digital CMOS DNA chip," in *Proc. IEEE Int. Symp. Circuits and Systems*, Kobe, Japan, 2005, pp. 2915–2918.

[14] A. Gore, S. Chakrabartty, S. Pal, and E. C. Alocilja, "A multichannel femtoampere-sensitivity potentiostat array for biosensing applications," *IEEE Trans. Circuits Syst. I, Reg. Papers*, vol. 53, pp. 2357–2363, 2006.

[15] M. Stanacevic, K. Murari, A. Rege, G. Cauwenberghs, and N. V. Thakor, "VLSI potentiostat array with oversampling gain modulation for wide-range neurotransmitter sensing," *IEEE Trans. Biomed. Circuits Syst.*, vol. 1, pp. 63–72, 2007.

[16] P. Weerakoon, E. Culurciello, K. G. Klemic, and F. J. Sigworth, "An integrated patch-clamp potentiostat with electrode compensation," *IEEE Trans. Biomed. Circuits Syst.*, vol. 3, pp. 117–125, 2009.

[17] M. H. Nazari, H. Mazhab-Jafari, L. Lian, A. Guenther, and R. Genov, "192-channel CMOS neurochemical microarray," in *Proc. Custom Integrated Circuits Conf.*, 2010, pp. 1–4.

[18] H. M. Jafari and R. Genov, "CMOS impedance spectrum analyzer with dual-slope multiplying ADC," in *Proc. Biomedical Circuits and Systems Conf.*, 2011, pp. 361–364.

[19] C. Yang, S. R. Jadhav, R. M. Worden, and A. J. Mason, "Compact low-power impedance-to-Digital converter for sensor array microsystems," *IEEE J. Solid-State Circuits*, vol. 44, pp. 2844–2855, 2009.

[20] S. Joo and R. B. Brown, "Chemical sensors with integrated electronics," *Chem. Rev.*, vol. 108, pp. 638–651, Feb. 2008.

[21] J. Voldman, M. L. Gray, and M. A. Schmidt, "Microfabrication in biology and medicine," *Annu. Rev. Biomed. Eng.*, vol. 1, pp. 401–425, 1999.

[22] R. Popovtzer, T. Neufeld, D. Biran, E. Z. Ron, J. Rishpon, and Y. Shacham-Diamand, "Novel integrated electrochemical nano-biochip for toxicity detection in water," *Nano. Lett.*, vol. 5, pp. 1023–1027, Jun. 2005.

[23] A. Bard and L. R. Faulkner, *Electrochemical Methods: Fundementals and Applications*. New York: Wiley, 1980.

[24] R. M. Wightman, "Voltammetry with microscopic electrodes in new domains," *Science*, vol. 240, pp. 415–420, Apr. 1988.

[25] S.-I. Park, S. B. Jun, S. Park, H. C. Kim, and S. J. Kim, "Application of a new Cl-plasma-treated Ag/AgCl reference electrode to micromachined glucose sensor," *IEEE Sensors J.*, vol. 3, pp. 267–273, Jun. 2003.

[26] L. Tymecki, E. Zwierkowska, and R. Koncki, "Screen-printed reference electrodes for potentiometric measurements," *Anal. Chim. Acta*, vol. 526, pp. 3–11, 2004.

[27] F. Moussy and D. J. Harrison, "Prevention of the rapid degradation of subcutaneously implanted Ag/AgCl reference electrodes using polymer coatings," *Anal. Chem.*, vol. 66, pp. 674–679, Mar. 1994.

[28] T. Matsumoto, A. Ohashi, and N. Ito, "Development of a micro-planar Ag/AgCl quasi-reference electrode with long-term stability for an amperometric glucose sensor," *Analytica Chimica Acta*, vol. 462, pp. 253–259, Jul. 2002.

[29] T. I. Valdes and F. Moussy, "A ferric chloride pre-treatment to prevent calcification of Nafion membrane used for implantable biosensors," *Biosens. Bioelectron.*, vol. 14, pp. 579–585, Jun. 1999.

[30] L. Lin, L. Xiaowen, W. A. Qureshi, and A. J. Mason, "CMOS amperometric instrumentation and packaging for biosensor array applications," *IEEE Trans. Biomed. Circuits Syst.*, vol. 5, pp. 439–448, 2011.

[31] M. H. Criqui, R. D. Langer, and D. M. Reed, "Dietary alcohol, calcium, and potassium. Independent and combined effects on blood pressure," *Circulation*, vol. 80, pp. 609–614, Sep. 1989.

[32] F. M. Sacks, L. P. Svetkey, W. M. Vollmer, L. J. Appel, G. A. Bray, D. Harsha, E. Obarzanek, P. R. Conlin, E. R. Miller, D. G. Simons-Morton, N. Karanja, P.-H. Lin, M. Aickin, M. M. Most-Windhauser, T. J. Moore, M. A. Proschan, and J. A. Cutler, "Effects on blood pressure of reduced dietary sodium and the dietary approaches to stop hypertension (DASH) diet," *New Eng. J. Med.*, vol. 344, pp. 3–10, 2001.

[33] A. Ottovaleitmannova and H. T. Tien, "Bilayer lipid-membranes—An experimental system for biomolecular electronic devices development," *Progre. Surf. Sci.*, vol. 41, pp. 337–445, Dec. 1992.

[34] A. Janshoff and C. Steinem, "Transport across artificial membranes-an analytical perspective," *Anal. Bioanal. Chem.*, vol. 385, pp. 433–451, Jun. 2006.

[35] E. Sackmann, "Supported membranes: Scientific and practical applications," *Science*, vol. 271, pp. 43–48, Jan. 1996.

[36] H. T. Tien, R. H. Barish, L. Q. Gu, and A. L. Ottova, "Supported bilayer lipid membranes as ion and molecular probes," *Anal. Sci.*, vol. 14, pp. 3–18, 1998.

[37] S. M. Schiller, R. Naumann, K. Lovejoy, H. Kunz, and W. Knoll, "Archaea analogue thiolipids for tethered bilayer lipid membranes on ultrasmooth gold surfaces," in *Angewandte Chemie-International Edition*. New York: Wiley, 2003, vol. 42, pp. 208–211.

[38] B. A. Cornell, V. L. B. BraachMaksvytis, L. G. King, P. D. J. Osman, B. Raguse, L. Wieczorek, and R. J. Pace, "A biosensor that uses ion-channel switches," *Nature*, vol. 387, pp. 580–583, Jun. 1997.

[39] V. Atanasov, N. Knorr, R. S. Duran, S. Ingebrandt, A. Offenhausser, W. Knoll, and I. Koper, "Membrane on a chip: A functional tethered lipid bilayer membrane on silicon oxide surfaces," *Biophys. J.*, vol. 89, pp. 1780–1788, Sep. 2005.

[40] C. A. Naumann, O. Prucker, T. Lehmann, J. Ruhe, W. Knoll, and C. W. Frank, "The polymer-supported phospholipid bilayer: Tethering as a new approach to substrate-membrane stabilization," *Biomacromolecules*, vol. 3, pp. 27–35, Jan. 2002.

[41] G. Krishna, J. Schulte, B. A. Cornell, R. J. Pace, and P. D. Osman, "Tethered bilayer membranes containing ionic reservoirs: Selectivity and conductance," *Langmuir*, vol. 19, pp. 2294–2305, Mar. 2003.

[42] B. Raguse, V. Braach-Maksvytis, B. A. Cornell, L. G. King, P. D. J. Osman, R. J. Pace, and L. Wieczorek, "Tethered lipid bilayer membranes: Formation and ionic reservoir characterization," *Langmuir*, vol. 14, pp. 648–659, Feb. 1998.

[43] S. Terrettaz, M. Mayer, and H. Vogel, "Highly electrically insulating tethered lipid bilayers for probing the function of ion channel proteins," *Langmuir*, vol. 19, pp. 5567–5569, Jul. 2003.

[44] R. Naumann, D. Walz, S. M. Schiller, and W. Knoll, "Kinetics of valinomycin-mediated $\mathbb{K}+$ ion transport through tethered bilayer lipid membranes," *J. Electroanal. Chem.*, vol. 550, pp. 241–252, Jul. 2003.

[45] N. Kohli, B. L. Hassler, L. Parthasarathy, R. J. Richardson, R. Y. Ofoli, R. M. Worden, and I. Lee, "Tethered lipid bilayers on electrolessly deposited gold for bioelectronic applications," *Biomacromolecules*, vol. 7, pp. 3327–3335, Dec. 2006.

[46] L. Becucci, R. Guidelli, C. Peggion, C. Toniolo, and M. R. Moncelli, "Incorporation of channel-forming peptides in a Hg-supported lipid bilayer," *J. Electroanal. Chem.*, vol. 576, pp. 121–128, Feb. 2005.

[47] B. L. Hassler, N. Kohli, J. G. Zeikus, I. Lee, and R. M. Worden, "Renewable dehydrogenase-based interfaces for bioelectronic applications," *Langmuir*, vol. 23, pp. 7127–7133, Jun. 2007.

[48] B. L. Hassler, M. Dennis, M. Laivenieks, J. G. Zeikus, and R. M. Worden, "Mutation of Tyr-218 to Phe in Thermoanaerobacter ethanolicus secondary alcohol dehydrogenase: Effects on bioelectronic interface performance," *Appl. Biochem. Biotechnol.*, vol. 143, pp. 1–15, 2007.

[49] S. J. Paddison, "Proton conduction mechanisms at low degrees of hydration in sulfonic acid-based polymer electrolyte membranes," *Annu. Rev. Mater. Res.*, vol. 33, pp. 289–319, Aug. 2003.

[50] W. Shinwari, D. Zhitomirsky, I. Deen, P. R. Selvaganapathy, J. Deen, and D. Landheer, "Microfabricated reference electrodes and their biosensing applications," *Sensors*, vol. 10, pp. 1679–1715, Mar. 2010.

[51] M. Wang, S. Yao, and M. Madou, "A long-term stable iridium oxide pH electrode," *Sens. Actuators B, Chem.*, vol. 81, pp. 313–315, 2002.

[52] R. K. Franklin, M. D. Johnson, K. A. Scottt, S. J. Ho, N. Hakhyun, D. R. Kipket, and R. B. Brown, "Iridium oxide reference electrodes for neurochemical sensing with MEMS microelectrode arrays," in *Proc. IEEE Int. Conf. Sensors*, Irvine, CA, Oct. 2005.

[53] M. Rehák, M. Šnejdárková, and M. Otto, "Self-assembled lipid bilayers as a potassium sensor," *Electroanal.* , vol. 5, pp. 691–694, 1993.

[54] E. Katz and I. Willner, "Kinetic separation of amperometric responses of composite redox-active monolayers assembled onto Au electrodes: Implications to the monolayers' structure and composition," *Langmuir*, vol. 13, pp. 3364–3373, Jun. 1997.

[55] R. Monošík, M. Stred'anský, and E. Šturdík, "Application of electrochemical biosensors in clinical diagnosis," *J. Clin. Lab. Anal.*, vol. 26, pp. 22–34, 2012.

[56] J.-C. Vidal, J. Espuelas, E. Garcia-Ruiz, and J.-R. Castillo, "Amperometric cholesterol biosensors based on the electropolymerization of pyrrole and the electrocatalytic effect of prussian-blue layers helped with self-assembled monolayers," *Talanta*, vol. 64, pp. 655–664, 2004.

Yue Huang (M'07) received the Ph.D. degree in electrical engineering from Michigan State University, East Lansing, in 2011.

His research focuses on biomedical microsystems, covering the areas of protein-based biosensors, site-directed mutagenesis, electrochemistry, analog/digital circuits and systems, microfabrication. In 2004, he joined the Advanced MicroSystems and Circuits Laboratory. In 2009, he founded LabSys LLC, an engineering research company. Currently, his research projects include electrochemical quartz microbalance instruments, bio-inspired adhesives, CMOS-superconductor integration, CMOS electrochemical sensor front-end, supercapacitor for bio-fuel cell hybrid power source and lab-on-CMOS integration for microsystems.

Ying Liu received the B.S. degree in bioengineering from the Dalian University of Technology, Dalian, Liaoning, China, and the M.S. degree in biochemical engineering from Tianjin University, Tianjin, China, in 2007 and 2009, respectively.

In her master project, she mainly focused on the application of lipidomics on studying the responses of Saccharomyces cerevisiae in different environment. Currently, she is a Ph.D. candidate in the the Department of Chemical Engineering and Materials Science, Michigan State University, East Lansing. Since 2009, her research interests have been focused on the study of the interactions of nanoparticles with biomimetic membranes.

Brian L. Hassler received the B.A. degree in chemical engineering from Michigan Technological University, Houghton, and the Ph.D. degree in chemical engineering from Michigan State University, East Lansing, in 2002 and 2009, respectively.

In 2011, he joined the Center for Electrochemical Engineering Research (CEER) at Ohio University, Athens, as the Facilities Manager. The CEER facilities include Raman and Fourier transform infrared spectroscopy, atomic force microscopy, and X-ray diffraction all capable of doing *in situ* electrochemistry. Currently, his research projects are focused on the production of hydrogen and nitrogen from ammonia and urea.

R. Mark Worden received the B.A. degree with a double major in chemistry and cell biology in 1979, the M.S. degree in chemical engineering in 1982, and the Ph.D. degree in chemical engineering in 1986, all from the University of Tennessee, Knoxville.

The research for his M.S. and Ph.D. degrees was conducted in the Bioprocess Engineering Group at Oak Ridge National Laboratory, Oak Ridge, TN. He became an Assistant Professor in the Department of Chemical Engineering and Materials Science at Michigan State University, East Lansing, in 1986, and was promoted to Associate Professor in 1991, and then Professor in 1998. His research program integrates recombinant-protein production, iocatalysis, and nanotechnology to develop new systems for bioproduction, biosensing, and bioremediation. His current projects include use of electrochemical sensor arrays for high-throughput biosensor systems and functional proteomics.

Andrew J. Mason (S'90-M'99-SM'06) received the B.S. degree in physics with highest distinction from Western Kentucky University, Bowling Green, in 1991, the B.S.E.E. degree with honors from the Georgia Institute of Technology, Atlanta, in 1992, and the M.S. and Ph.D. degrees in electrical engineering from the University of Michigan, Ann Arbor, in 1994 and 2000, respectively.

From 1999 to 2001, he was an Assistant Professor at the University of Kentucky, Lexington. In 2001, he joined the Department of Electrical and Computer Engineering at Michigan State University, East Lansing, where he is currently an Associate Professor. His research explores mixed-signal circuits and microfabricated structures for integrated microsystems in biomedical and environmental monitoring applications. Current projects include wearable/implantable electrochemical and bioelectronic sensors systems, microfabricated electrochemical sensor arrays, array signal processing algorithms and hardware, and post-CMOS integration of sensing, instrumentation, and microfluidics.

Dr. Mason serves on the Sensory Systems and Biomedical Circuits and Systems Technical Committees of the IEEE Circuits and Systems Society and on the technical program committee for several IEEE conferences and workshops. He is an Associate Editor of the IEEE TRANSACTIONS ON BIOMEDICAL CIRCUITS AND SYSTEMS and was co-General Chair of the 2011 IEEE BioCAS Conference. He is a recipient of the 2006 Michigan State University Teacher-Scholar Award and the 2010 Withrow Award for Teaching Excellence.